Applied Physics, Material Sciences, and Engineering Journal
ISSN 3065-1425
Volume 13 Issue 1
January-March 2025
Impact Factor: 8.13
Enquiry: contact@continentalpub.online
Published by Continental Publication | https://cspjournals.org/index.php/apmsej

ACCELERATED DISCOVERY OF DECHLORINATION CATALYSTS: A STUDY OF MXENES VIA COMPUTATIONAL SCREENING

Tomáš Ivan Novák
Department of Physics, Faculty of Science, University of Ostrava, 30. dubna 22, 701 03 Ostrava, Czech Republic

Abstract: *Chlorinated hydrocarbons are persistent environmental pollutants with severe health impacts, prompting the need for efficient and scalable remediation strategies. MXenes, a class of two-dimensional materials with tunable surface chemistries, show promise as catalytic agents for pollutant degradation. In this study, density functional theory (DFT) is employed to investigate the adsorption and dechlorination of trichloroethylene (TCE) on variously terminated MXenes. The results indicate that $Ti_2C(OH)_2$ and $V_2C(OH)_2$ enable spontaneous TCE dechlorination with low reaction barriers (<1 eV). Notably, even a partial substitution (17%) of –O terminations by –OH on non-defected Ti_2CO_2 leads to efficient dechlorination, yielding dichloroethylene and HCl. MXenes with single terminal vacancies further enhance catalytic activity, exhibiting barriers as low as 0.1 eV. Additionally, other chlorinated pollutants such as lindane and DDT also undergo spontaneous dechlorination on pristine $Ti_2C(OH)_2$, demonstrating the broader applicability of MXenes. These findings underscore the potential of MXenes as efficient and versatile catalysts for the degradation of chlorinated hydrocarbons, providing valuable mechanistic insights for their practical deployment in environmental remediation.*

Keywords: *MXenes, Dechlorination, Chlorinated hydrocarbons, Density functional theory (DFT).*

1. Introduction

Due to their high chemical stability and effectiveness, chlorinated hydrocarbons are a class of compounds widely used in industrial applications, including solvents, pesticides, and chemical intermediates. However, these properties contribute to their environmental persistence, making them significant pollutants [1]. Their resistance to natural degradation processes leads to accumulation in soil and groundwater, posing severe environmental and health risks [2]. Prominent examples of such pollutants include dichlorodiphenyltrichloroethane (DDT) and lindane. Although their use has been banned or restricted in many countries due to their toxicity and environmental persistence, legacy contamination remains a significant concern. Historically employed to control vector-borne diseases like malaria, DDT is known for its bioaccumulation in the food chain and its detrimental effects on wildlife and human health [3, 4]. Lindane, an isomer of hexachlorocyclohexane, has applications in agriculture and pharmaceuticals but is similarly associated with environmental persistence and significant toxicity. Studies have linked lindane exposure to

Copyright: © 2025 Continental Publication

Vol. 13 No. 1 | Imp. Factor: 8.13
DOI: https://doi.org/10.5281/zenodo.15845815
neurological and reproductive health issues [5, 6]. The persistence and toxicity of these compounds necessitate advanced remediation strategies to mitigate their impact effectively.
© 2025 The Author(s). Published by IOP Publishing Ltd
Trichloroethylene (TCE), a volatile chlorinated hydrocarbon, is widely used as an industrial solvent in applications such as metal degreasing, paint removal, and chemical synthesis. Improper handling and disposal have made TCE a prominent environmental contaminant, particularly in soil and groundwater [7]. Exposure to TCE has been linked to severe health risks, including liver and kidney damage, respiratory issues, and increased risks of cancer, including liver cancer and non-Hodgkin's lymphoma. The environmental mobility of TCE, combined with its persistence, makes it a critical target for remediation efforts.

Traditional remediation techniques, including pump-and-treat, air stripping, and soil vapor extraction, have shown limited efficiency, high costs, and environmental drawbacks. Pump-and-treat methods are time-consuming and often fail to achieve complete decontamination, while air stripping requires careful management to prevent secondary air pollution from volatilized contaminants. Soil vapor extraction is constrained by soil permeability and may not fully address contamination in less accessible zones. These challenges underscore the need for innovative, efficient, and sustainable technologies for the remediation of chlorinated hydrocarbons.

In recent years, nanotechnology has offered promising solutions for pollutant degradation. Nanoscale zero-valent iron (nZVI) has emerged as a widely studied material for TCE remediation due to its high surface area and reactivity. nZVI facilitates reductive dechlorination, breaking TCE into less harmful compounds like ethene and chloride ions. However, challenges such as nanoparticle aggregation, reduced mobility in subsurface environments, and potential environmental impacts have limited the effectiveness of nZVI. Recent advancements, such as sulfidation and nitridation, have enhanced the stability and reactivity of nZVI particles [8, 9]. Sulfidated nanoparticles primarily exhibit amorphous structures, while nitridated nanoparticles crystallize in the Fe_4N phase, significantly improving TCE degradation performance.

Emerging materials, such as MXenes—a class of two-dimensional transition metal carbides and nitrides—are perspective to offer an alternative approach to environmental remediation. MXenes are characterized by unique properties, including high electrical conductivity, hydrophilicity, and tunable surface chemistry, which make them suitable for advanced applications. Studies have demonstrated the ability of MXenes, such as $Ti_3C_2T_x$, to enhance photocatalytic pollutant degradation and to effectively remove contaminants like heavy metals, organic dyes, and pharmaceuticals through adsorption and ion exchange mechanisms [10–20]. Despite challenges in synthesis and functionalization, MXene-based materials have shown significant potential for water purification and sustainable remediation efforts.

This study explores the interaction of TCE and other chlorinated hydrocarbons, including DDT and lindane, with functionalized MXenes. Using density functional theory (DFT) calculations, we investigated the adsorption energies, dechlorination mechanisms, and surface reactivity of MXenes terminated with –F, –O, and –OH groups and mixed terminations. Both pristine and defected MXenes were analyzed to provide a comprehensive understanding of the mechanisms underlying pollutant

Copyright: © 2025 Continental Publication

Vol. 13 No. 1 | Imp. Factor: 8.13
DOI: https://doi.org/10.5281/zenodo.15845815

capture and degradation on MXenes. Our findings aim to advance the application of MXenes as efficient materials for environmental remediation and contribute to developing innovative solutions for mitigating the impact of chlorinated hydrocarbons. These compounds were selected to represent structurally and functionally distinct classes of chlorinated hydrocarbons: TCE as a small, volatile solvent; DDT as a persistent aromatic pesticide; and lindane as a cyclic, highly chlorinated compound. This diversity allows us to assess the general applicability of MXene-based materials across a broad range of chlorinated hydrocarbon pollutants relevant to environmental remediation.

2. Computational methods

All calculations were performed using the Vienna *ab initio* Simulation Package [21, 22]. The electronic structure of atoms was described using the projector-augmented wave (PAW) method, with electronic exchange and correlation terms treated within the framework of the generalized gradient approximation (GGA) to DFT using the Perdew–Burke–Ernzerhof (PBE) density functional [23]. Dispersion corrections were incorporated into the PBE energy using the DFT-D3 scheme with Becke–Johnson damping to account for van der Waals interactions [24]. The plane-wave kinetic energy cutoff was set to 500 eV for all calculations (for convergence of adsorption energies, see table S1 in Supporting material). A force convergence criterion of 0.001 eVÅ^{-1} was applied for ionic relaxation, while an electronic self-consistent field convergence criterion of 10^{-7} eV was used. Brillouin zone sampling used a Γ-centered 2×2×1 k-point grid. Since all pristine MXenes studied are non-magnetic in their ground state and adsorbed molecules are closed-shell, spin-polarized calculations were not used for ground-state adsorption energy calculations.

However, spin-polarization was included in the energy barrier calculations.

We modeled slabs as optimized orthogonal supercells. To construct an orthogonal supercell $(\mathbf{a}',\mathbf{b}')$ from the hexagonal unit cell given by $\mathbf{a} = (a,0)$ and $\mathbf{b} = (-\frac{a}{2}, \frac{\sqrt{3}a}{2})$, where a is the MXene lattice constant, we applied a transformation $(\mathbf{a}',\mathbf{b}')=(\mathbf{a},\mathbf{b})\begin{pmatrix}3 & 0\\ 2 & 4\end{pmatrix}$ (for schematic representation see figure S1 in the supplementary material). A vacuum region of 30 Å in the z-direction was included to minimize interactions between periodic images. Adsorption energies of TCE molecules were calculated using the equation: $E_{ads} = E_{complex} - (E_{slab} + E_{mol})$, where $E_{complex}$ is the total electronic energy of the relaxed complex consisting of the molecule adsorbed on the slab, E_{slab} is the total energy of the relaxed bare slab, and E_{mol} is the total energy of the isolated molecule. Given the planar structure and physisorptive character of the TCE molecule, we considered the most physically relevant and stable initial adsorption geometry, which led to consistent, weakly interacting configurations across all systems. The reported adsorption energies correspond to these optimized structures. The energy barriers for the dechlorination of TCE were computed using the climbing image nudged elastic band (NEB) method [25]. This approach allowed the identification of transition states and the calculation of the minimum energy paths for the reactions studied.

3. Results and discussion

We modeled three types of nonmagnetic carbide MXenes: Sc_2C, Ti_2C, and V_2C, terminated with different functional groups. These MXenes represent a class of 2D transition metal carbides known for their tunable surface chemistry and promising adsorption properties, making them suitable for environmental and catalytic applications. Several distinct MXenes (including mixed terminations)

Copyright: © 2025 Continental Publication

Vol. 13 No. 1 | Imp. Factor: 8.13
DOI: https://doi.org/10.5281/zenodo.15845815

were examined to assess their interaction with TCE, an environmentally hazardous organic compound. We note that Ti_3C_2 is currently the most widely studied and experimentally available MXene. To address its relevance, we modeled the interaction of TCE with $Ti_3C_2O_2$ and found that the adsorption behavior and energies are nearly identical to those on Ti_2CO_2 (see figure S2 and table S2 in the supplementary material). Since both materials share the same surface termination and similar surface chemistry, we focus on Ti_2C in this work for simplicity, lower computational demands, and to enable a consistent comparison with Sc_2C and V_2C. The Sc_2CO_2 was excluded from our study due to instability. Optimized *a* lattice constants of studied MXenes are 3.23 Å, and 3.27 Å for Sc_2CF_2 and $Sc_2C(OH)_2$, 3.00 Å, 3.01 Å, and 3.02 Å for Ti_2CF_2, Ti_2CO_2, and $Ti_2C(OH)_2$, and 2.92 Å, 2.88 Å, and 2.94 Å for V_2CF_2, V_2CO_2, and $V_2C(OH)_2$. For Ti_2C with mixed terminations, a = 3.02 Å was used. We note that there are several possible positions of terminal groups in MXenes. We chose the trigonal structure with the terminal group in the hollow position, which is the most energetically favorable for studied MXenes [26].

3.1. Adsorption energies

We studied eight MXenes in their fully terminated form (further called pristine) and with a single vacancy in their termination groups. Interestingly, two MXenes terminated with –OH, $Ti_2C(OH)_2$ and $V_2C(OH)_2$, demonstrate spontaneous dechlorination of TCE without any energetic barrier even in their pristine form. Conversely, $Sc_2C(OH)_2$ and Ti_2CF_2 demonstrated a propensity for spontaneous dissociation of TCE, but only when a vacancy was present in their termination groups.

This manuscript section delves into the stable adsorption configurations of TCE on the tested MXenes, providing insights into the nature of the physisorbed interactions. Subsequent sections of our study elaborate on detailed discussions of the dissociation mechanisms of TCE.

3.1.1. Pristine MXenes

All stable adsorption configurations on pristine MXenes are depicted in figure 1, with the distances between TCE atoms and surface atoms annotated in red. Table 1 provides a comprehensive summary of the adsorption energies, which show slight variations depending on the MXene composition and its termination.

Pure DFT energies for –O and –F terminations yielded positive adsorption energies, indicating weak or non-favorable interactions. However, when dispersion corrections are included, adsorption energies become consistently negative, highlighting the critical role of van der Waals forces in stabilizing TCE adsorption. This behavior indicates that the interaction of TCE with fully terminated –O and –F surfaces is primarily physisorptive in nature, dominated by long-range dispersion forces rather than chemical bonding. GGA functionals like PBE do not adequately capture these van der Waals interactions, leading to an

Table 1. Adsorption energies E_{ads} (in eV) of TCE on pristine functionalized MXenes calculated using DFT+D3 (including decomposition to DFT and D3 parts).

MXene	Sc_2C		Ti_2C		V_2C	
Termination	$-F_2$	$-(OH)_2$	$-F_2$	$-O_2$	$-F_2$	$-O_2$

Copyright: © 2025 Continental Publication

Vol. 13 No. 1 | Imp. Factor: 8.13
DOI: https://doi.org/10.5281/zenodo.15845815

*E*DFTads	−0.46	−0.56	−0.50	−0.58	−0.47	−0.61
+D3	0.04	−0.06	0.05	0.07	0.05	0.05
$E\mathrm{DFT}_{\mathrm{ads}}$	−0.50	−0.48	−0.55	−0.65	−0.52	−0.66
$E\mathrm{D}_{\mathrm{ads}}3$						

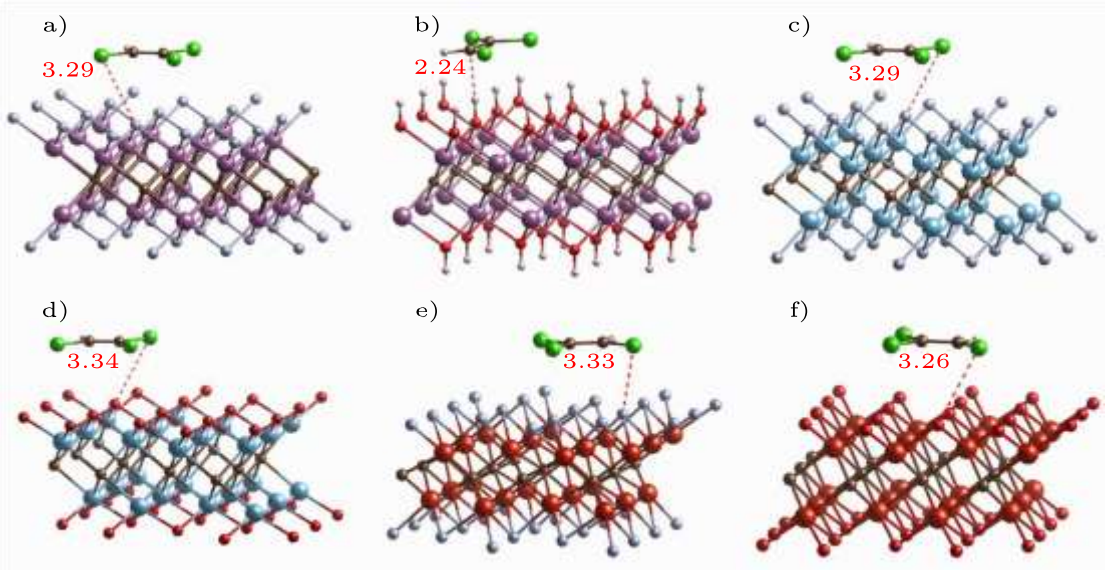

Figure1. Adsorption of TCE molecule on various MXenes:(a) Sc_2CF_2, (b) $Sc_2C(OH)_2$, (c) Ti_2CF_2, (d) Ti_2CO_2, (e) V_2CF_2, and V_2CO_2. Distances are in Å, and the colors of atoms are: carbon-brown, oxygen-red, fluorine-grey, hydrogen-white, chlorine-green, scandium-pink, titanium-blue, and vanadium-crimson.

underestimation of adsorption energies. The substantial negative contribution from the D3 correction (table 1) confirms that dispersion is the driving factor behind stable adsorption on these terminations. $Sc_2C(OH)_2$ is the only pristine MXene in our study terminated with –OH where the stable adsorption place was observable. This suggests a nuanced relationship between the metal center's electronic structure and the reactivity of the termination groups. This finding highlights the importance of both metal choice and functionalization in tuning adsorption properties for targeted applications.

The adsorption configuration character was remarkably consistent across all tested MXenes, featuring planar adsorption of TCE. The distances between the molecule and the surfaces, particularly for MXenes terminated with –F and –O, ranged from 3.26 to 3.34 Å, as illustrated in figure 1.

3.1.2. Defected MXenes

To deepen our understanding of the interactions between TCE and MXenes, we explored the adsorption characteristics on defected MXenes, where one terminal group was deliberately removed (single terminal vacancy). This intentional modification of the surface chemistry markedly influenced adsorption behaviors, with some defected systems demonstrating notably enhanced adsorption capabilities.

Crucially, among the systems studied, two exhibited a transition from stable adsorption to spontaneous dissociation of TCE: $Sc_2C(OH)_2$ and Ti_2CF_2. This shift highlights the significant impact of terminal vacancies on chemical reactivity.

Copyright: © 2025 Continental Publication

Vol. 13 No. 1 | Imp. Factor: 8.13
DOI: https://doi.org/10.5281/zenodo.15845815

Figure 2 presents all stable adsorptions on single terminal vacancy MXenes, where a noticeable shift from planar to a more perpendicular orientation of TCE on the MXene can be observed. This alteration suggests adapting the adsorption mechanism in response to the modified electronic environment of the single terminal vacancy MXenes.

Table 2 summarizes the adsorption energies, showing an apparent increase in magnitude compared to non-defected systems, indicating stronger interactions post-defection. Additionally, the distances between the molecule and the surface atoms have decreased across all single terminal vacancy systems (figure 2). Notably, for single terminal vacancy Sc_2CF_2 and Ti_2CO_2, the shortest distances between the molecule and the exposed metal atoms are now observed. In contrast, the closest interactions remain between the molecule and the terminal groups for both vanadium-defected MXenes.

3.2. TCE dechlorination

The interaction between TCE and both pristine and single terminal vacancy MXenes illuminates their potential for catalytic applications, especially in reactions involving chlorinated hydrocarbons. Table 3 presents the reaction energies associated with the dissociation of TCE (C_2HCl_3) into its fragments (C_2HCl_2 + Cl), providing insight into the energetic feasibility of the process. Table 3 deliberately excludes instances of spontaneous dissociation, focusing instead on controlled dissociation dynamics.

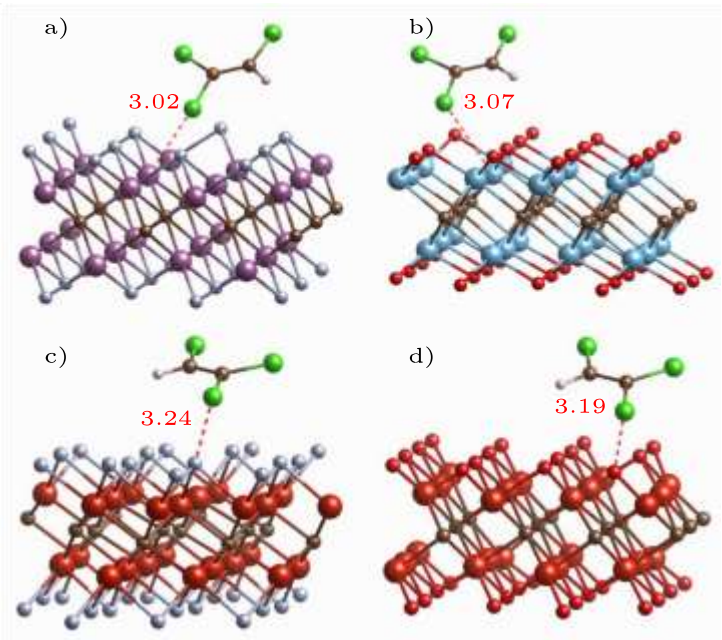

Figure2. Adsorption of TCE molecule on various single terminal vacancy MXenes: (a) Sc_2CF_2, (b) Ti_2CO_2, (c) V_2CF_2, and (d) V_2CO_2. Distances are in Å, and the colors of atoms are: carbon-brown, oxygen-red, fluorine-grey, hydrogen-white, chlorine-green, scandium-pink, titanium-blue, and vanadium-crimson.

Table 2. Adsorption energies E_{ads} (in eV) of TCE on single terminal vacancy MXenes calculated using DFT+D3 (including decomposition to DFT and D3 parts).

Surface	Sc_2C	Ti_2C	V_2C	
Termination	$-F_2$	$-O_2$	$-F_2$	$-O_2$

Copyright: © 2025 Continental Publication

Vol. 13 No. 1 | Imp. Factor: 8.13
DOI: https://doi.org/10.5281/zenodo.15845815

*E*DFTads	−0.81	−0.97	−0.57	−0.77
+D3	−0.18	−0.17	0.04	0.02
$E\text{DFT}_{ads}$	−0.63	−0.80	−0.61	−0.79
$E\text{D}_{ads}3$				

Pristine MXenes with –O and –F terminations exhibit high positive energy differences between non-dissociated and dissociated TCE forms, ranging between 2.65 eV and 3.23 eV. This disparity indicates a weaker stabilization of the dissociated TCE species on these MXenes. The trend observed across pristine MXenes terminated with –O and –F underscores their limited efficacy in facilitating dechlorination, as the dissociated forms are energetically unfavorable.

Conversely, single terminal vacancy MXenes show significantly narrower reaction energies, underscoring the pivotal role of surface defects in stabilizing dissociated species. Notably, these differences often turn negative, indicating that the dissociation process is exothermic and thermodynamically favorable. This enhanced stabilization is particularly evident in single terminal vacancy systems such as Sc_2CF_2, Ti_2CO_2, and V_2CO_2. However, V_2CF_2 stands out with a positive energy difference, suggesting that its dissociation process is endothermic.

Missing reaction energy for $Sc_2C(OH)_2$ in table 3 is due to the inability to find stable adsorption configuration of C_2HCl_2 + Cl on both pristine and defected $Sc_2C(OH)_2$. Subsequent spontaneous reactions are present, such as the formation of dichloroethylene (DCE) (CH_2Cl_2) with a highly exothermic nature, which suggests robust catalytic activity. The mechanism of these reactions is deeply studied in section 3.3 in this manuscript.

3.2.1. Spontaneous TCE dechlorination

The hydroxyl-terminated Ti_2C and V_2C demonstrated remarkable reactivity towards TCE, primarily through the spontaneous dissociation of the molecule upon interaction with these MXenes. This capability highlights the exceptional chemical reactivity conferred by hydroxyl terminations, rendering them highly effective in capturing and potentially degrading hazardous organic compounds such as TCE. Notably, both MXenes spontaneously facilitated dechlorination even in their pristine states.

Table 3. Reaction energies E_{react} associated with the dissociation of TCE (C_2HCl_3) into its fragments C_2HCl_2 + Cl (in eV) on pristine and single terminal vacancy MXenes calculated using DFT+D3.

MXene	Sc_2C	Ti_2C		V_2C	
Termination	$-F_2$	$-F_2$	$-O_2$	$-F_2$	$-O_2$
$E\text{pristine}_{react}$	3.23	2.68	2.68	2.66	2.65
$E\text{defected}_{react}$	0.70	—	1.55	0.08	−1.33
	–				
		–			

Copyright: © 2025 Continental Publication

Vol. 13 No. 1 | Imp. Factor: 8.13
DOI: https://doi.org/10.5281/zenodo.15845815

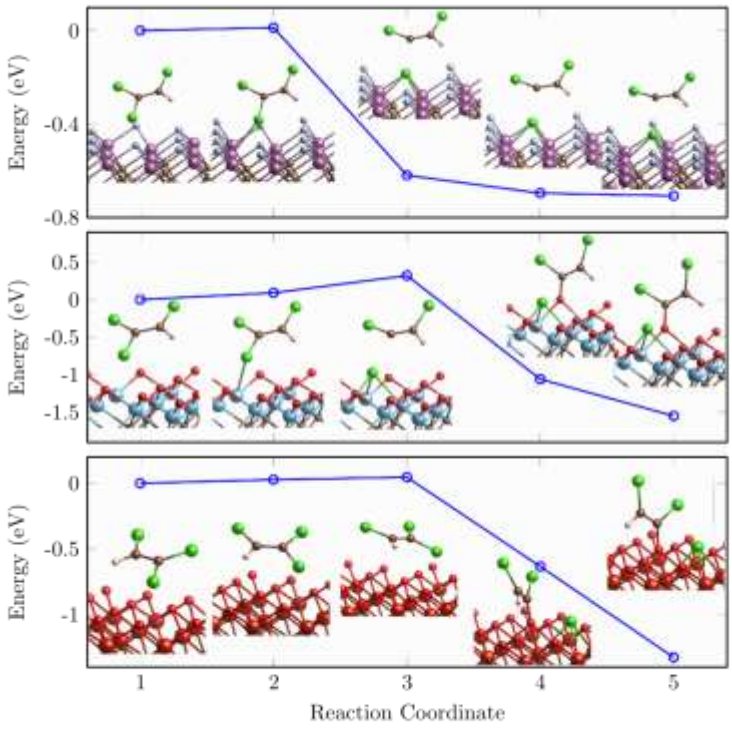

Figure 3. NEB calculations of dissociation of TCE on single terminal vacancy Sc_2CF_2 (top), Ti_2CO_2 (center), and V_2CO_2 (bottom).

Similarly, single terminal vacancy $Sc_2C(OH)_2$ displayed comparable dechlorination behavior. In contrast, single terminal vacancy Ti_2CF_2 also enabled spontaneous dechlorination of TCE, albeit to a lesser extent, involving the removal of one chlorine atom from TCE molecule, without spontaneous subsequent reactions visible in –OH terminated surfaces. This distinction underscores the impact of different surface terminations and defects on the catalytic efficiency and specificity of MXene materials.

3.2.2. Barrier-driven TCE dechlorinations

To further decipher the dissociation mechanisms of TCE on MXenes, we applied the NEB method to determine the reaction coordinates for dechlorination on single terminal vacancy MXenes where stable adsorption was observed. Our study focused exclusively on energetically favorable reactions, encompassing Sc_2CF_2, Ti_2CO_2, and V_2CO_2. Figure 3 presents the corresponding reaction profiles.

For Sc_2CF_2, the activation energy at the transition state is exceptionally low, calculated to be just 0.06 eV. This indicates a highly favorable dechlorination pathway, positioning Sc_2CF_2 as a promising material for catalytic dechlorination applications. In comparison, other –F-terminated MXenes with single vacancies show varying behaviors: while Ti_2CF_2 enables spontaneous TCE dechlorination, V_2CF_2 exhibits an endothermic reaction profile (table 3). These differences emphasize the pivotal role of the metal atom in determining the effectiveness of TCE dechlorination, even on defective surfaces.

The oxygen-terminated MXenes, Ti_2CO_2 and V_2CO_2, both exhibit exothermic reaction profiles, which are indicative of energetically favorable dechlorination processes (figure 3). The activation barriers are 0.36 eV for Ti_2CO_2 and a notably lower 0.06 eV for V_2CO_2, suggesting these materials are auspicious for catalytic dechlorination.

Copyright: © 2025 Continental Publication

Vol. 13 No. 1 | Imp. Factor: 8.13
DOI: https://doi.org/10.5281/zenodo.15845815

These findings underscore the transformative impact of surface defects in modulating the reactivity of MXene materials. Pristine MXenes often struggle to stabilize dissociated TCE molecules; however, introducing single terminal vacancies can dramatically alter the surface chemistry, fostering localized environments conducive to exothermic reactions and reducing activation barriers. Among the systems evaluated, single terminal vacancy Sc_2CF_2 and oxygen-terminated V_2CO_2 emerge as the most effective catalysts for TCE dechlorination, combining thermodynamic favorability with minimal kinetic resistance.

3.3. Ti_2C mixed composition

The most reactive MXenes for TCE dechlorination are those terminated with –OH groups, as exemplified by $Ti_2C(OH)_2$ and $V_2C(OH)_2$, where dechlorination occurs spontaneously without any energetic barrier. This highlights the exceptional catalytic potential of hydroxyl terminations, driven by their ability to engage in hydrogen bonding and electron transfer. However, real-world MXenes are likely to feature mixed terminations. To better understand their catalytic behavior under realistic conditions, we focus on Ti_2C with mixed –O and –OH terminations, given that –O is the predominant termination [26].

Our investigation assessed the adsorption and reactivity of Ti_2C with varying proportions of –OH groups. This approach not only simulates more realistic environmental conditions but also helps identify the minimum –OH coverage required for effective catalytic performance in TCE dechlorination. A key question was whether the presence of even a small number of –OH groups could maintain high reactivity.

In our computational model, we ensured that the opposite surface of the Ti_2C layer, which did not interact with TCE, was terminated purely with –O groups to simulate realistic experimental scenarios. Each side of the MXene in the computational cell contained a total of 12 termination groups. Mixed terminations on the reactive surface were systematically varied, with –O:–OH ratios ranging from 1:11 to 11:1. The corresponding chemical formulas were $Ti_2CO_{1.08}(OH)_{0.92}$ and $Ti_2CO_{1.92}(OH)_{0.08}$, respectively. For simplicity, we refer to these MXenes by their –OH coverage, e.g. 8%–OH.

Our results revealed stable adsorption of TCE on Ti_2C with –OH coverages ranging from 8% to 75 %. Spontaneous dissociation of TCE occurred until the –OH coverage decreased below 83%. Below this threshold, adsorption became dominated by van der Waals forces, leading to physisorbed TCE with DFT+D3-calculated adsorption energies between −0.79 and −0.94 eV. This suggests that while –OH terminations are essential for chemical reactivity, MXenes with low –OH content retain strong physical interactions with TCE.

To study the favorability of TCE dissociation on mixed termination MXenes, we considered the adsorption of dissociated TCE products (C_2HCl_2 + Cl). The presence of –OH groups facilitated the spontaneous formation of DCE ($C_2H_2Cl_2$) and hydrochloric acid (HCl). Notably, even at low –OH coverages (17%–OH), the reaction remained energetically favorable, with reaction energy of −0.89 eV and −0.64 eV for 25%–OH and 17%–OH, respectively. These findings indicate that a small proportion of –OH terminations can sustain dechlorination processes under realistic conditions.

We proposed a reaction mechanism and used the NEB method to calculate the reaction barriers. For a representative 17%–OH, the mechanism involves five key steps:

Copyright: © 2025 Continental Publication

Vol. 13 No. 1 | Imp. Factor: 8.13
DOI: https://doi.org/10.5281/zenodo.15845815

1. Dissociation of a hydrogen atom from the surface (17%–OH → 8%–OH + H).
2. Addition of the dissociated hydrogen atom to the TCE molecule, partially breaking the double bond ($C_2HCl_3 + H \rightarrow C_2H_2Cl_3$). This configuration was confirmed as a transition state.
3. Dissociation of a chlorine atom from the TCE molecule, forming the DCE molecule ($C_2H_2Cl_3 \rightarrow C_2H_2Cl_2 + Cl$).
4. Dissociation of another hydrogen atom from the surface (8%–OH → Ti_2CO_2 + H).
5. Formation of HCl from the free hydrogen and chlorine atom (Cl + H → HCl).

The NEB model for this process is shown in figure 4. The mixed termination groups enhance the process by providing active sites for hydrogen abstraction and bond rearrangement. The transition state exhibits significant structural distortion of the TCE molecule. One carbon atom remains bonded to hydrogen and chlorine, preserving partial similarity to pristine TCE, while the second carbon forms new bonds with two chlorine atoms and hydrogen derived from the MXene surface. This geometry indicates partial cleavage of the TCE double bond, a critical step for dissociation. Bader charge analysis reveals a charge shift of approximately 1.7 e from one carbon atom to the other, indicating intense polarization of the C–C bond in the transition state. However, since all molecules during this reaction remain neutral, the reaction proceeds via a radical mechanism rather than an electrophilic process. In particular, hydrogen atoms abstracted from the MXene surface retain their electrons, suggesting a homolytic bond cleavage rather than charge separation.

The calculated barriers for these processes are 0.81 eV (25%–OH) and 0.97 (17%–OH figure 4) eV. Although these barriers are relatively high, we must note that we modeled reactions involving only two or three –OH groups on the surfaces, with no accessible metal atoms. Despite the limited –OH coverage, the MXenes demonstrate strong reactivity toward TCE. We conclude that even a small coverage of –OH groups on MXene surfaces can drive significant reactions with TCE.

Copyright: © 2025 Continental Publication

Vol. 13 No. 1 | Imp. Factor: 8.13
DOI: https://doi.org/10.5281/zenodo.15845815

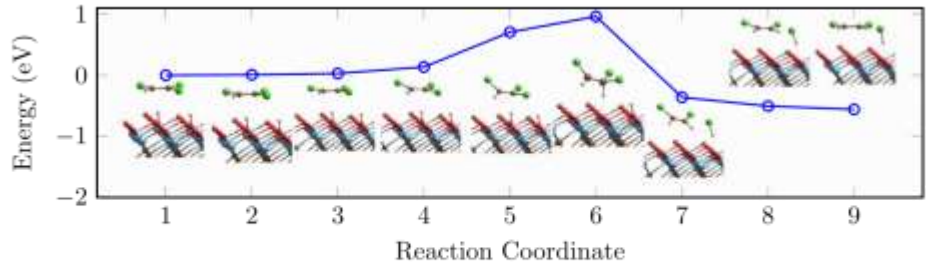

Figure 4. NEB calculation of TCE dissociation on mixed-termination Ti_2C 17%−OH.

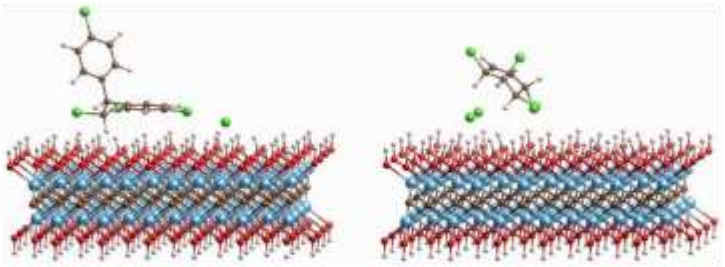

Figure 5. Adsorption of DDT (left) and lindane (right) on $Ti_2C(OH)_2$ surface. The colors of atoms are: carbon-brown, oxygen-red, hydrogen-white, chlorine-green, and titanium-blue.

In summary, mixed termination groups on Ti_2C enable effective dechlorination of TCE, driven by the unique catalytic properties of –OH terminations. These findings reinforce the potential of MXenes in environmental remediation and demonstrate the critical role of surface terminations in tuning their catalytic performance.

3.4. Other chlorinated hydrocarbons

To generalize our conclusions about the reactivity of hydroxyl-terminated MXenes ($Ti_2C(OH)_2$) toward chlorinated hydrocarbons, we extended our study by investigating the interaction of DDT and lindane with the $Ti_2C(OH)_2$. Both molecules exhibited spontaneous dissociation of chlorine atoms upon adsorption on the MXene surface without any discernible energetic barrier. This observation is consistent with the high reactivity observed for TCE on similar materials.

In the case of DDT, the interaction led to the dissociation of a single chlorine atom. The vacancy created by this dissociation was immediately stabilized by a hydrogen atom from the surface, highlighting the unique ability of $Ti_2C(OH)_2$ to promote the substitution of surface-bound groups during the reaction. This mechanism effectively minimizes the energy cost of the reaction, underscoring the thermodynamic favorability of dechlorination on the MXene. The reaction was even more pronounced for lindane, a molecule characterized by a higher chlorine content, with two chlorine atoms dissociating spontaneously (figure 5).

These results suggest that the reactivity of $Ti_2C(OH)_2$ is not limited to TCE but extends to structurally diverse chlorinated hydrocarbons. Both DDT and Lindane represent complex molecules with multiple chlorine atoms and distinct chemical structures, yet their behavior on the $Ti_2C(OH)_2$ demonstrates similar trends of spontaneous dechlorination. This points to a broader capability of hydroxyl-

Copyright: © 2025 Continental Publication

Vol. 13 No. 1 | Imp. Factor: 8.13
DOI: https://doi.org/10.5281/zenodo.15845815
terminated MXenes to act as effective agents for the degradation of chlorinated hydrocarbons. The observed reactivity can be attributed to the synergistic effect of the hydroxyl terminations' high chemical potential and the MXene surface's strong affinity for polarizable halogen atoms.

Given the environmental persistence and toxicity of compounds like DDT and lindane, these findings have significant implications for applying MXenes in environmental remediation. The ability to spontaneously cleave C–Cl bonds without requiring external energy input positions $Ti_2C(OH)_2$ as a promising material for detoxifying persistent organic pollutants. Moreover, the versatility of $Ti_2C(OH)_2$ in facilitating reactions with different chlorinated hydrocarbons underscores its potential utility in treating a wide range of chlorinated contaminants in various environmental contexts.

Future studies should focus on elucidating the mechanistic details of the lindane and DDT dechlorination process. Additionally, experimental validation of the computational results will be crucial to confirming the practical feasibility of $Ti_2C(OH)_2$ as a remediation agent for chlorinated hydrocarbons. These investigations could pave the way for developing tailored MXene materials optimized for specific environmental applications, enhancing their utility in sustainable remediation strategies.

4. Conclusion

This study comprehensively analyzes TCE's interactions and dechlorination mechanisms on MXenes, highlighting their potential as advanced remediation materials for addressing persistent organic pollutants. Using DFT calculations, we systematically investigated the interactions of TCE with three MXenes Sc_2C, Ti_2C, and V_2C functionalized with –F, –O, and –OH terminations and mixed compositions.

Our findings reveal that MXenes, particularly $Ti_2C(OH)_2$ and $V_2C(OH)_2$, facilitate spontaneous dechlorination processes, demonstrating exceptional reactivity and versatility. Following the realistic ratio of MXene surface termination, we prove that non-defected Ti_2CO_2 with just 17% of –O terminations substituted by –OH group still possesses strongly favorable TCE remediation and the dechlorination of TCE with spontaneous forming of DCE and HCl after barrier of <1 eV. Furthermore, single terminal vacancy MXenes, terminated with –O and –F, possess the TCE reductive ability with a very low barrier <0.1 eV in some cases. Lindane and DDT, another representatives of chlorinated hydrocarbons, spontaneously dechlorate on pristine $Ti_2C(OH)_2$.

This work underscores the transformative potential of MXenes in environmental remediation, offering a scalable and efficient alternative to conventional technologies. By addressing key challenges such as pollutant persistence and incomplete remediation, MXenes could serve as a cornerstone for sustainable and practical solutions to mitigate the impact of hazardous contaminants on global ecosystems.

Data availability statement

The data cannot be made publicly available upon publication because they are not available in a format that is sufficiently accessible or reusable by other researchers. The data that support the findings of this study are available upon reasonable request from the authors.

Acknowledgments

This article has been produced with the financial support of the European Union under the LERCO Project Number CZ.10.03.01/00/22_003/0000003 via the Operational Programme Just Transition.

Copyright: © 2025 Continental Publication

Vol. 13 No. 1 | Imp. Factor: 8.13
DOI: https://doi.org/10.5281/zenodo.15845815
Calculations were performed at IT4Innovations National Supercomputing Center (e-INFRA CZ, ID:90254).

References

Algaradah, M. M. (2024). MXene-based adsorbent materials for pollutants removal from water: Current challenges and future prospects. Inorganic Chemistry Communications, 161, 112113. https://doi.org/10.1016/j.inoche.2024.112113

Alvarez-Pedrerol, M., Ribas-Fitó, N., Torrent, M., Carrizo, D., Garcia-Esteban, R., Grimalt, J. O., & Sunyer, J. (2008). Thyroid disruption at birth due to prenatal exposure to β-hexachlorocyclohexane. Environment International, 34, 737–740. https://doi.org/10.1016/j.envint.2008.01.002

Alyasi, H., Wahib, S., Gomez, T. A., Rasool, K., & Mahmoud, K. A. (2024). The power of MXene-based materials for emerging contaminant removal from water—a review. Desalination, 586, 117913. https://doi.org/10.1016/j.desal.2024.117913

Aparicio, J. D., Lacalle, R. G., Artetxe, U., Urionabarrenetxea, E., Becerril, J. M., Polti, M. A., Garbisu, C., & Soto, M. (2021). Successful remediation of soils with mixed contamination of chromium and lindane: Integration of biological and physico-chemical strategies. Environmental Research, 194, 110666. https://doi.org/10.1016/j.envres.2020.110666

Blöchl, P. (1994). Projector augmented-wave method. Physical Review B, 50(24), 17953–17979. https://doi.org/10.1103/PhysRevB.50.17953

Brumovský, M., Oborná, J., Micić, V., Malina, O., Kašlík, J., Tunega, D., Kolos, M., Hofmann, T., Karlický, F., & Filip, J. (2022). Iron nitride nanoparticles for enhanced reductive dechlorination of trichloroethylene. Environmental Science & Technology, 56(7), 4425–4433. https://doi.org/10.1021/acs.est.1c07614

Chen, S., Meng, Y., Wang, X., Liu, D., Meng, X., Wang, X., & Wu, G. (2024). Hollow tubular MnO_2/MXene (Ti_3C_2, Nb_2C, and V_2C) composites as high-efficiency absorbers with synergistic anticorrosion performance. Carbon, 218, 118698. https://doi.org/10.1016/j.carbon.2023.118698

Dorsey, E. R., et al. (2023). Trichloroethylene: An invisible cause of Parkinson's disease? Journal of Parkinson's Disease, 13(2), 203–215. https://doi.org/10.3233/JPD-230038

Copyright: © 2025 Continental Publication

Vol. 13 No. 1 | Imp. Factor: 8.13
DOI: https://doi.org/10.5281/zenodo.15845815

Grimme, S., Ehrlich, S., & Goerigk, L. (2011). Effect of the damping function in dispersion corrected density functional theory. Journal of Computational Chemistry, 32, 1456–1465. https://doi.org/10.1002/jcc.21759

Hao, Z., Zhou, J., Lin, S., Lan, D., Li, H., Wang, H., Liu, D., Gu, J., Wang, X., & Wu, G. (2024). Customized heterostructure of transition metal carbides as high-efficiency and anti-corrosion electromagnetic absorbers. Carbon, 228, 119323. https://doi.org/10.1016/j.carbon.2023.119323

Henkelman, G., Uberuaga, B. P., & Jónsson, H. (2000). A climbing image nudged elastic band method for finding saddle points and minimum energy paths. The Journal of Chemical Physics, 113(22), 9901–9904. https://doi.org/10.1063/1.1329672

Jatoi, A. S., Mubarak, N. M., Hashmi, Z., Solangi, N. H., Karri, R. R., Tan, Y. H., Mazari, S. A., Koduru, J. R., & Alfantazi, A. (2023). New insights into MXene applications for sustainable environmental remediation. Chemosphere, 313, 137497. https://doi.org/10.1016/j.chemosphere.2022.137497

Kolos, M., Tunega, D., & Karlický, F. (2020). A theoretical study of adsorption on iron sulfides towards nanoparticle modeling. Physical Chemistry Chemical Physics, 22, 23258–23268. https://doi.org/10.1039/D0CP03487D

Kong, A., Sun, Y., Peng, M., Gu, H., Fu, Y., Zhang, J., & Li, W. (2021). Amino-functionalized MXenes for efficient removal of Cr(VI). Colloids and Surfaces A: Physicochemical and Engineering Aspects, 617, 126388. https://doi.org/10.1016/j.colsurfa.2021.126388

Kresse, G., & Joubert, D. (1999). From ultrasoft pseudopotentials to the projector augmented-wave method. Physical Review B, 59, 1758–1775. https://doi.org/10.1103/PhysRevB.59.1758

Kumar, J. A., Prakash, P., Krithiga, T., Amarnath, D. J., Premkumar, J., Rajamohan, N., Vasseghian, Y., Saravanan, P., & Rajasimman, M. (2022). Methods of synthesis, characteristics and environmental applications of MXene: A comprehensive review. Chemosphere, 286, 131607. https://doi.org/10.1016/j.chemosphere.2021.131607

Liu, D., Liu, J., Li, C., Ji, Y., Han, Y., Xue, Z., Lv, Q., Chen, J., Wang, Y., & Li, H. (2024). Tailoring surface terminals on MXene enables high-efficiency electromagnetic absorption. Carbon, 228, 119392. https://doi.org/10.1016/j.carbon.2023.119392

McCarty, P. L. (2010). Groundwater contamination by chlorinated solvents: History, remediation technologies and strategies. In H. F. Stroo & C. H. Ward (Eds.), In situ remediation of

Copyright: © 2025 Continental Publication

Vol. 13 No. 1 | Imp. Factor: 8.13
DOI: https://doi.org/10.5281/zenodo.15845815

chlorinated solvent plumes (pp. 1–28). Springer. https://doi.org/10.1007/978-1-4419-1401-9_1

My Tran, N., Thanh Hoai Ta, Q., Sreedhar, A., & Noh, J.-S. (2021). $Ti_3C_2T_x$ MXene playing as a strong methylene blue adsorbent in wastewater. Applied Surface Science, 537, 148006. https://doi.org/10.1016/j.apsusc.2020.148006

Novotný, M., Tkáčová, K., & Karlický, F. (2024). The effect of mixed termination composition in Sc, Ti and V-based MXenes. Physical Chemistry Chemical Physics, 26, 25514–25523. https://doi.org/10.1039/D4CP01223G

Perdew, J. P., Burke, K., & Ernzerhof, M. (1996). Generalized gradient approximation made simple. Physical Review Letters, 77, 3865–3868. https://doi.org/10.1103/PhysRevLett.77.3865

Purnomo, A. S., Mori, T., Kamei, I., & Kondo, R. (2011). Basic studies and applications on bioremediation of DDT: A review. International Biodeterioration & Biodegradation, 65, 921–930. https://doi.org/10.1016/j.ibiod.2011.07.003

Raheem, I., Mubarak, N. M., Karri, R. R., Solangi, N. H., Jatoi, A. S., Mazari, S. A., Khalid, M., Tan, Y. H., Koduru, J. R., & Malafaia, G. (2023). Rapid growth of MXene-based membranes for sustainable environmental pollution remediation. Chemosphere, 311, 137056. https://doi.org/10.1016/j.chemosphere.2022.137056

Shahzad, A., Rasool, K., Miran, W., Nawaz, M., Jang, J., Mahmoud, K. A., & Lee, D. S. (2017). Two-dimensional $Ti_3C_2T_x$ MXene nanosheets for efficient copper removal from water

Copyright: © 2025 Continental Publication